RESEARCH ARTICLE

QbD-Based Formulation, Optimization and *In-vitro* Antifungal Evaluation of Sulconazole-Loaded Nanosponges Encapsulated in Hydrogel

Jhansi Rani Mallam[1*], Nagaraju Ravouru[2]

[1]*Dr. Anji Reddy College of Pharmacy, Piduguralla-522413, Andhra Pradesh, India*
[2]*Institute of Pharmaceutical Technology, Sri Padmavati Mahila Visvavidyalayam (Women's University) Tirupati-517502, Andhra Pradesh, India*

Received: 7th May, 2025; Revised: 29th Jun, 2025; Accepted: 14th Jul, 2025; Available Online: 25th Sep, 2025

ABSTRACT
Using a QbD framework, this study developed and optimized a nanosponge-based hydrogel system for topical delivery of Sulconazole. CCD was used to identify the ideal concentrations of Ethyl Cellulose (polymer) and PVA (surfactant), with particle size and entrapment efficiency as critical responses. Nanosponges were produced via emulsion solvent evaporation and evaluated using FTIR, DSC, SEM, zeta potential, and UV spectroscopy. The optimized formulation, F11, achieved a size of 265.7 nm, zeta potential of −23.54 mV, PDI of 0.286, and high %EE and %DL. Hydrogel prepared using Carbopol 940 exhibited appropriate pH, viscosity, spreadability, and sustained drug release up to 12 hours. Antifungal evaluation confirmed potent MIC and MFC values against *C. albicans* and *A. niger*, with F11 outperforming both the pure drug and commercial cream in all microbiological assays.
Keywords: Sulconazole, Nanosponges, Hydrogel, QbD, Antifungal activity, Controlled release
How to cite this article: Jhansi Rani Mallam, Nagaraju Ravouru. QbD-Based Formulation, Optimization, and *In-vitro* Antifungal Evaluation of Sulconazole-Loaded Nanosponges Encapsulated in Hydrogel. International Journal of Drug Delivery Technology. 2025;15(3):966-74. doi: 10.25258/ijddt.15.3.9
Source of support: Nil.
Conflict of interest: None

INTRODUCTION

Sulconazole nitrate is an imidazole-derived broad-spectrum antifungal agent primarily used to treat superficial fungal infections such as dermatophytosis and candidiasis. It acts by inhibiting ergosterol biosynthesis, a critical component of fungal cell membranes, thus disrupting membrane integrity and leading to cell death[1]. Sulconazole exhibits potent activity against dermatophytes, yeasts, and molds, including *Candida albicans* and *Aspergillus niger*[2,3]. However, conventional topical formulations often suffer from poor skin penetration and limited retention time, which compromises therapeutic efficacy[3,4]. These limitations necessitate the development of advanced drug delivery systems that can enhance skin permeability, sustain drug release, and provide prolonged antifungal activity at the site of infection[5,6]. As porous polymeric carriers, nanosponges facilitate the encapsulation of various drug types, boosting solubility and stability while allowing for sustained drug delivery[7]. When incorporated into hydrogels, nanosponges combine the advantages of nanoparticulate systems with the hydrophilic, bioadhesive, and occlusive properties of gel matrices. This dual system enhances topical delivery by ensuring prolonged drug retention at the site of application and reducing dosing frequency[8]. The use of hydrogels also improves patient compliance due to their non-greasy nature and ease of application[9,10].

To date, numerous works like nanoparticulate gels[11], methods for in vitro antifungal evaluation[12], topical delivery systems such as nanosponges and nanogels[13-15], QbD-optimized nanosponge formulations[16,17], cyclodextrin-based nanosponges[18], voriconazole-loaded nanosponges for topical use[19], and solid lipid nanoparticles[20].

MATERIALS AND METHODS

Materials

A gift sample of Sulconazole was provided by Hetero Drugs, Hyderabad. Ethyl Cellulose was received from Lee Pharma Limited, Visakhapatnam. All additional chemicals, including polyvinyl alcohol and solvents of analytical grade, were procured from SDFCL, Mumbai.

Experimental Design

A Central Composite Design under RSM was selected to optimize the formulation variables affecting Sulconazole nanosponges.

Ethyl Cellulose and Polyvinyl Alcohol served as independent inputs, with the outputs being particle size and % entrapment efficiency. The experimental design included 13 formulations (F1–F13) analyzed via Design Expert 10.0.3.1.

Formulation of Sulconazole-loaded NS

Sulconazole-loaded nanosponges (F1–F13) were prepared via the emulsion solvent evaporation method as per CCD specifications. Formulations were prepared by dissolving EC and Sulconazole in dichloromethane and adding the solution dropwise to a PVA aqueous phase under 1000 rpm stirring for 2 hours. After vacuum filtration and drying at 40°C for 24 hours, samples were stored in a desiccator. Table 2 presents the formulation compositions.

Characterization of Sulconazole-loaded Nanosponges

**Author for Correspondence: jhansi92789@gmail.com*

Table 1: Design Summary of Independent and Dependent Variables used in RSM-CCD

Variable Type	Parameter	Symbol	Low Level	High Level
Independent Variable	Ethyl Cellulose (mg)	X1	100	300
Independent Variable	Polyvinyl Alcohol (mg)	X2	100	300
Dependent Variable	Particle Size (nm)	Y1		
Dependent Variable	Entrapment Efficiency (%)	Y2		

Particle Size, Zeta Potential, and Polydispersity Index (PDI)

The Malvern Nano ZS Zetasizer was employed to determine the average particle size, zeta potential, and PDI of the optimized Sulconazole nanosponges. Dilution with distilled water was performed before analysis to ensure reliable scattering data. These measurements offered insights into the physical stability, size uniformity, and electrostatic repulsion between particles within the formulation.

Entrapment Efficiency and Drug Loading Capacity

To evaluate drug entrapment and loading, 50 mg of the nanosponge sample was mixed with 10 mL of pH 6.8 phosphate buffer and stirred until complete dissolution. The supernatant was then analyzed at 234 nm using UV spectrophotometry. Entrapment efficiency and drug loading were calculated using standard equations involving total and free drug content.

Table 2: Sulconazole-loaded nanosponges formulations

F-code	X_1 (mg)	X_2 (mg)	Y_1 (nm)	Y_2 (%)
F1	341.421	200	360	81.21
F2	100	300	335	82.68
F3	200	200	280	83.72
F4	200	58.5786	350	82.11
F5	58.5786	200	343	82.23
F6	200	200	275	83.78
F7	200	341.421	365	81.24
F8	100	100	326	82.14
F9	300	300	365	82.19
F10	200	200	275	83.86
F11	200	200	265	84.48
F12	200	200	278	83.91
F13	300	100	340	82.78

FTIR and DSC Analysis

To determine compatibility between Sulconazole and excipients, FTIR spectra were recorded from 4000 to 400 cm^{-1} using potassium bromide pellets. Thermal behavior was assessed using DSC (DSC-PYRIS-1), with

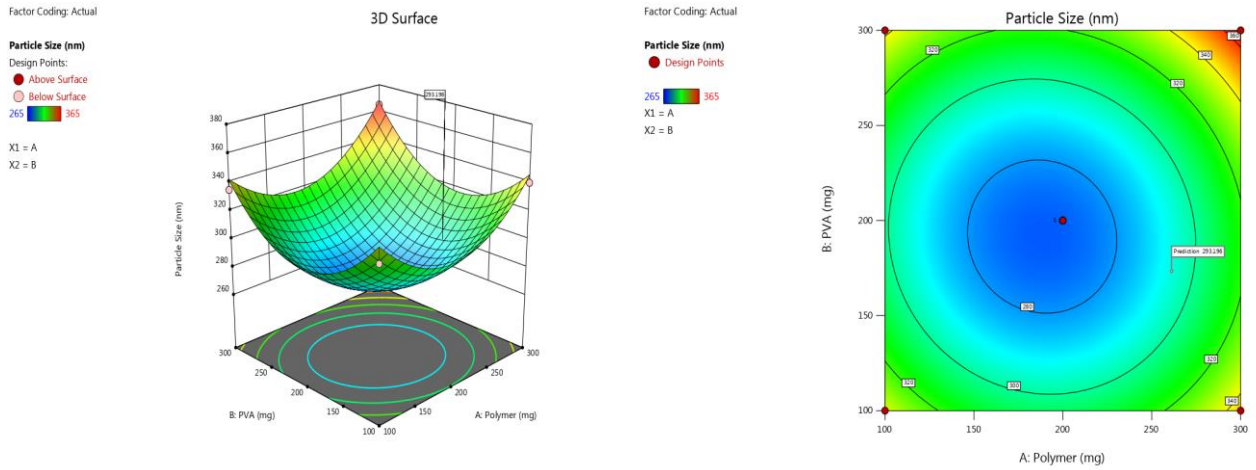

Figure 1: Response plot depicting the impact of X1 and X2 on particle size (Y1)

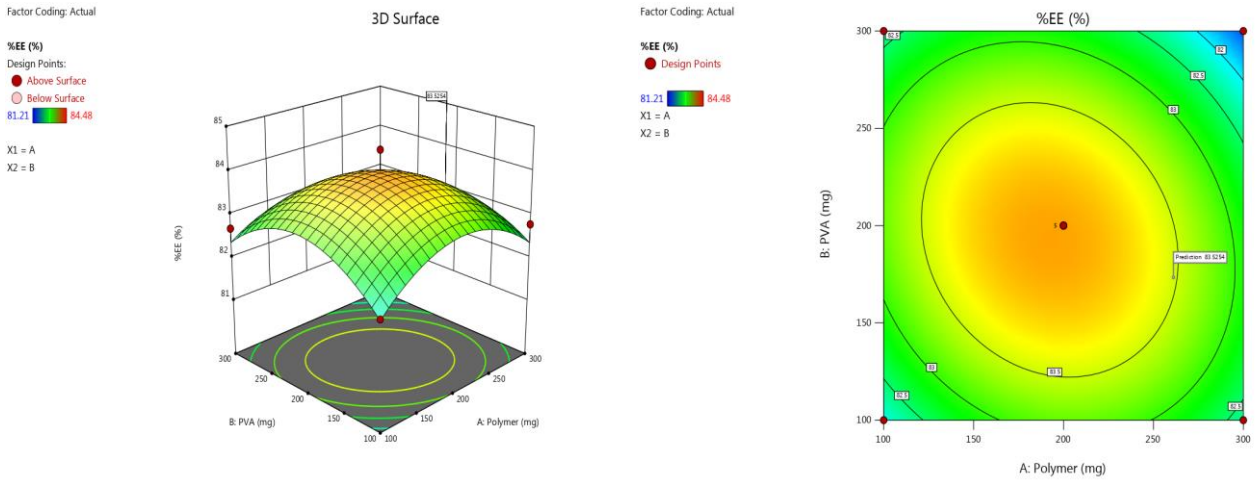

Figure 2: Response plot depicting impact of X1 and X2 on entrapment efficiency

Results

			Size (d.nm):	% Intensity:	St Dev (d.n...
Z-Average (d.nm):	265.7	Peak 1:	295.5	100.0	79.85
PdI:	0.286	Peak 2:	0.000	0.0	0.000
Intercept:	0.954	Peak 3:	0.000	0.0	0.000
Result quality :	Good				

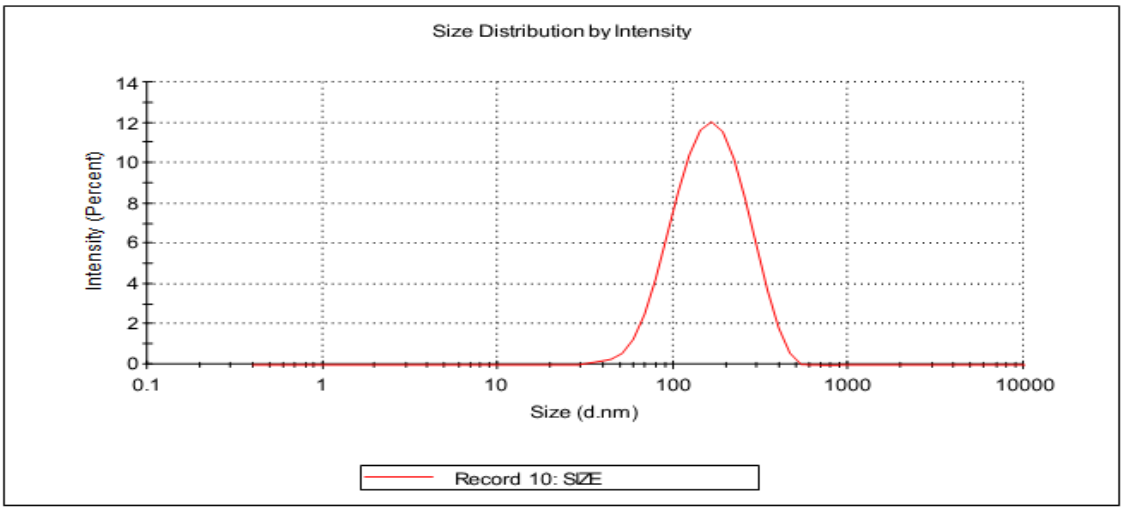

Figure 3: Particle size of F11 batch

Results

			Mean (mV)	Area (%)	St Dev (mV)
Zeta Potential (mV):	-23.54	Peak 1:	-23.54	100.0	7.28
Zeta Deviation (mV):	7.28	Peak 2:	0.00	0.0	0.00
Conductivity (mS/cm):	0.0628	Peak 3:	0.00	0.0	0.00
Result quality :	Good				

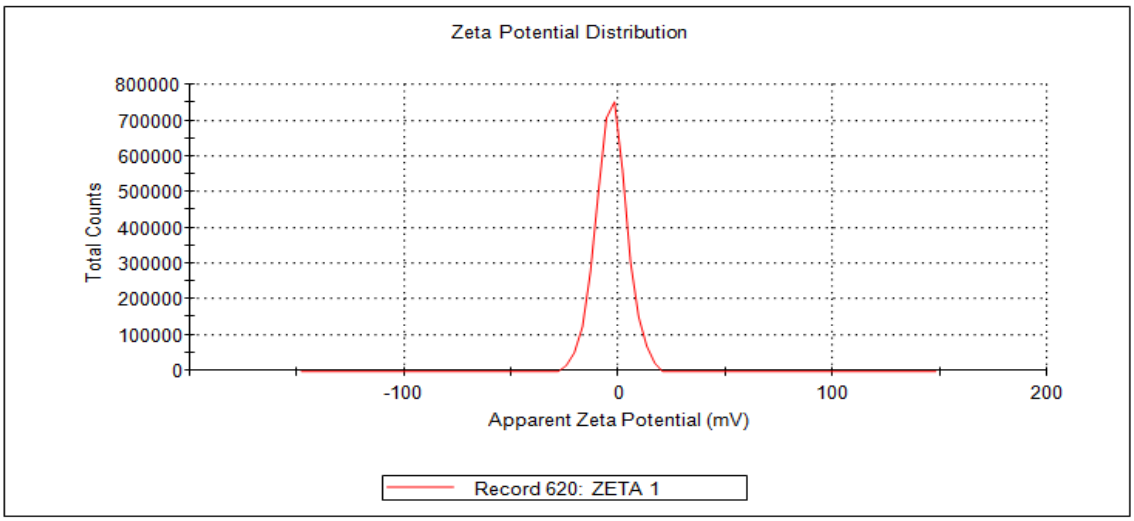

Figure 4: Zeta Potential of F11 batch

samples heated from ambient temperature at a rate of 10 °C/min under a nitrogen purge. The combined use of FTIR and DSC confirmed the physical integrity and stability of Sulconazole in the formulation[21-24].

Scanning Electron Microscopy Analysis

A Carl Zeiss scanning electron microscope, coupled with Oxford EDX, was utilized in high-vacuum mode to visualize the surface structure of Sulconazole nanosponges[25].

In-vitro Drug Release Study

A USP Type-II paddle apparatus was used to assess the drug release of Sulconazole nanosponges, using 900 mL of pH 6.8 phosphate buffer at 37 ± 0.2°C and 100 rpm. Diffusion bags holding 10 mg of drug were tested, and samples were

withdrawn at hourly intervals up to 12 hours and measured at 234 nm.

Hydrogel Formulation and Evaluation

Preparation of Sulconazole-Loaded Nanosponge Hydrogel

The optimized nanosponges were incorporated into a Carbopol 940-based hydrogel. The gelling agent was pre-soaked in water overnight. Propylene glycol was added as a penetration enhancer, followed by dispersion of nanosponges (equivalent to 10 mg of drug). The mixture was stirred on a magnetic stirrer at 400 rpm for 20 minutes to ensure uniform distribution[26, 27].

pH and Drug Content Evaluation

The hydrogel's pH was measured using a digital pH meter (Digisun Electronics, Hyderabad) to ensure skin compatibility, aiming for a range between 6.0 and 8.0. For drug content analysis, 1 g of gel was dissolved in 100 mL of phosphate buffer (pH 6.8), and a 5 mL sample was further diluted to 25 mL. Sulconazole content was quantified using UV spectrophotometry at 234 nm, and the percentage of drug content was calculated using the formula: (Actual / Theoretical) × 100.

Viscosity Measurement and Spreadability Study

The viscosity of the Sulconazole hydrogel was measured using a Brookfield viscometer (Prime Rheometer DV 1) at 100 rpm and 25°C to assess its consistency and suitability for topical application.

Spreadability was evaluated using the sliding plate method, where 1 g of gel was placed between two glass plates under a fixed weight of 125 g, and the time taken for plate separation was recorded as a measure of the gel's ease of application.

In-vitro Diffusion Study

Using the Franz diffusion apparatus, in vitro permeation of Sulconazole hydrogel was studied across cellulose membranes. The receptor compartment contained pH 6.8 buffer, maintained at 32 ± 0.5°C. Following the application of 1 g gel, samples were withdrawn at 30-minute intervals and analyzed at 234 nm.

In-vitro Antifungal Activity

Agar Well Diffusion Method

Using the agar well diffusion technique, antifungal effectiveness of F11 Nanogel, plain Sulconazole, and marketed cream was evaluated against *Candida albicans* and *Aspergillus niger*. Fungal strains were cultured on SDA plates, into which 100 µL of each drug sample (equivalent to 2 µg) was dispensed. Following 48 hours of incubation at 28 ± 2°C, inhibition zones were determined using a Vernier calliper[28].

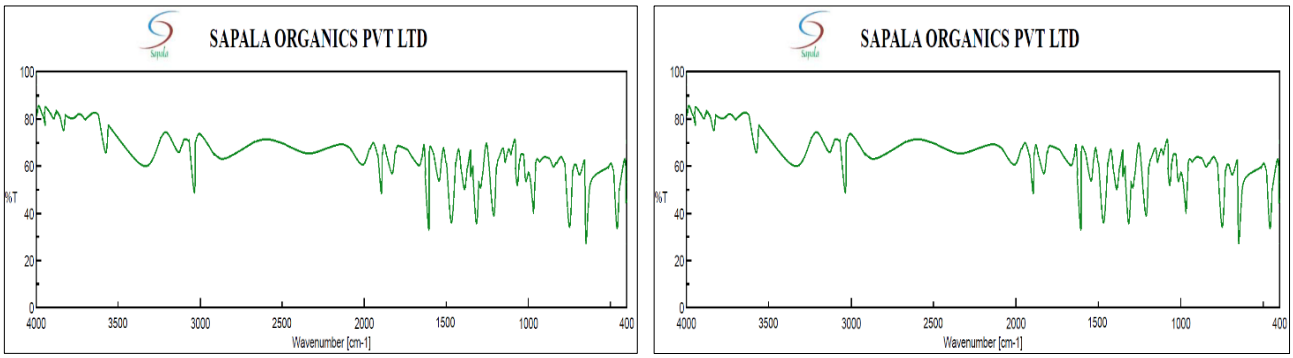

Figure 5: FTIR spectra of Drug and Physical Mixture

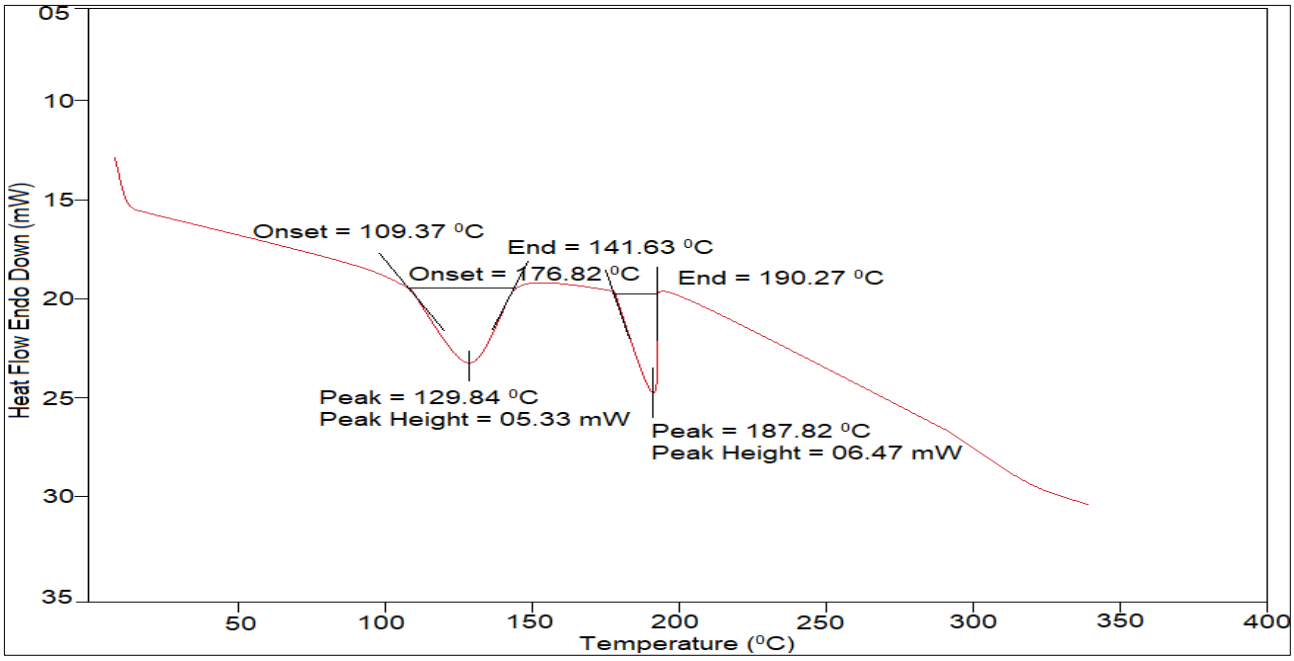

Figure 6: DSC of F11 batch

Table 3: Model Fit Statistics

Models	R^2	R^2 (Adj)	R^2 (Pred)	Residual Standard Error	%RSD
Response -Y_1	0.9702	0.9489	0.8289	8.79	2.75
Response -Y_2	0.8535	0.7488	0.1102	0.5330	0.6438

Table 4: Evaluation of Variance in Experimental Data

Source	Squared Deviations	d.f	MS	Test Statistic	Probability Value	
Model	17636.88	5	3527.38	45.60	< 0.0001	Sig.
A-Polymer	578.71	1	578.71	7.48	0.0291	
B-PVA	381.06	1	381.06	4.93	0.0619	
AB	64.00	1	64.00	0.8274	0.3933	
A^2	8619.41	1	8619.41	111.44	< 0.0001	
B^2	10151.23	1	10151.23	131.24	< 0.0001	
Residual	541.43	7	77.35			
Lack of Fit	408.23	3	136.08	4.09	0.1037	Sig. N.S.
Pure Error	133.20	4	33.30			
Cor Total	18178.31	12				

Table 5: Evaluation of Variance in Experimental Data

Source	Squared Deviations	d.f	MS	Test Statistic	Probability Value	
Model	11.58	5	2.32	8.15	0.0078	Sig.
A-Polymer	0.2088	1	0.2088	0.7351	0.4196	
B-PVA	0.2049	1	0.2049	0.7213	0.4238	
AB	0.3192	1	0.3192	1.12	0.3243	
A^2	5.98	1	5.98	21.07	0.0025	
B^2	6.28	1	6.28	22.10	0.0022	
Residual	1.99	7	0.2841			
Lack of Fit	1.62	3	0.5387	5.79	0.0615	Sig. N.S.
Pure Error	0.3724	4	0.0931			
Cor Total	13.57	12				

Broth Micro Dilution Assay

Broth microdilution was performed following the CLSI M27-A3 protocol, where serial dilutions (16–0.0625 µg/mL) of each formulation were tested in RPMI-1640 medium against 10^4 CFU/mL fungal cells. MIC and MFC were identified post-incubation at 35 ± 2°C based on turbidity and subculture results[29,30].

RESULTS AND DISCUSSION

Optimization

Both Y1 and Y2 responses were best described by a quadratic model, with elevated R^2 values suggesting a statistically significant and reliable fit. As shown in Table 3, Y1 exhibited an R^2 of 0.9702 and Y2 showed an R^2 of 0.8535, confirming the suitability of the model for optimization.

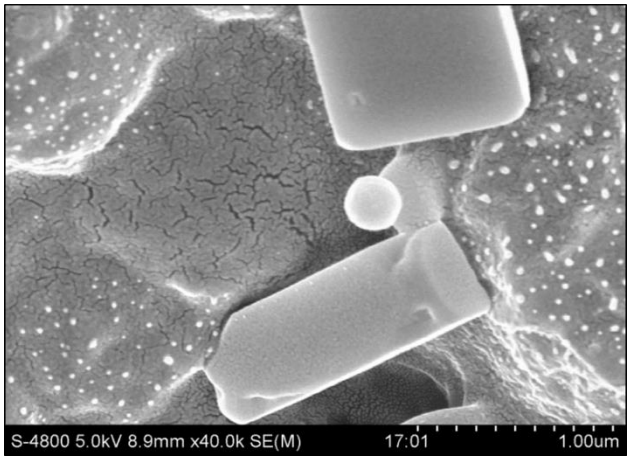

Figure 7: SEM image of F11 batch

Regression Equations:

$Y1=+274.60+8.51*A+6.90*B+4.00*AB+35.20*A^2+38.20*B^2$ ---------- (1)

$Y2=+83.95-0.1616*A-0.1600*B-0.2825*AB-0.9275*A^2-0.9500*B^2$ ---------- (2)

The polynomial regression equations Y1 and Y2 describe the relationships between the dependent variables (Y1and Y2) and the independent variables (A and B), including their linear, interaction (AB), and quadratic effects. These equations demonstrate how changes in A and B, individually and in combination, influence Y1and Y2, with quadratic terms accounting for non-linear variations.

Model Assessment for Dependent Variables

The ANOVA results (Table 4) for particle size (Y1) showed that the quadratic model was statistically significant ($p < 0.0001$), with polymer concentration (A), and especially its squared term (A^2), having a significant influence on the response. Similarly, Table 5 shows that the model for entrapment efficiency (Y2) was also significant ($p = 0.0078$), with both A^2 and B^2 terms contributing meaningfully to the model ($p < 0.01$). Lack-of-fit was found to be non-significant for both responses, confirming the adequacy of the models.

Response Surface Plot Analysis

As shown in Figures 1 and 2, a balanced concentration of X1 and X2 significantly influenced particle size, with formulation F11 (200 mg each of X1 and X2) yielding the smallest size (265 nm). This suggests that equal ratios of

Table 6: % EE and %DL of batches

Batch Code	%EE	DL (%)
F1	81.31±0.08	71.25±0.10
F2	82.12±0.11	74.92±0.12
F3	81.11±0.07	78.41±0.14
F4	82.11±0.12	70.25±0.16
F5	82.23±0.14	77.42±0.18
F6	80.17±0.15	80.32±0.20
F7	82.24±0.17	77.32±0.09
F8	83.41±0.14	74.11±0.11
F9	82.19±0.16	80.53±0.13
F10	83.86±0.15	75.21±0.15
F11	86.24±0.11	83.89±0.17
F12	83.90±0.13	70.93±0.19
F13	82.17±0.15	71.11±0.21

Table 7: *In-vitro* release profile of optimized nanosponges

Time (Hours)	F11	Pure Drug
0	0	0
2	28.08 ± 0.04	32.42 ± 0.03
4	51.56 ± 0.03	65.16 ± 0.07
6	69.61 ± 0.02	83.25 ± 0.05
8	81.97 ± 0.09	99.42 ± 0.06
10	89.26 ± 0.03	---
12	98.03 ± 0.01	-----

polymer and surfactant promote uniform nanosponge formation and prevent aggregation, making F11 the optimized formulation

The response surface plot of Ethyl Cellulose concentration (X_1) and PVA (X_2) (%EE) (Y_2). The highest %EE was observed in F11 (84.48%). These formulations generally had smaller particle sizes, suggesting a possible correlation between smaller particle size and higher encapsulation efficiency.

Table 8: Characterization of Nanosponges Gel

S. No.	Formulation code	pH value of NS	pH value of NS gel	Viscosity (cps)
11	F11	6.21 ± 0.01	5.85 ± 0.09	1968 ± 2.19

Table 9: Characterization of Nanosponges Gel

S. No.	Formulation code	Drug Content (%)	Spreadability (%)
1	F11	91.41 ± 0.19%	93.49 ± 1.09%

Table 10: Drug Diffusion Profile of Sulconazole Nanogel

Time (Hours)	Hydrogel (F11)
0	0
2	15.14 ± 1.36
4	32.32 ± 2.41
6	56.68 ± 1.69
8	79.28 ± 2.32
10	85.29 ± 2.56
12	95.38 ± 2.96

Table 11: Zone of Inhibition of *C. albicans and A. niger*

Formulation	*C. albicans*	*A. niger*
	ZOI (mm)	ZOI (mm)
Sulconazole Nanosponges (F11)	21.3 ± 0.5	19.7 ± 0.6
Pure Sulconazole (2 µg)	18.9 ± 0.4	17.8 ± 0.5
Marketed Sulconazole Cream	20.3 ± 0.4	18.9 ± 0.4
Placebo Gel (No drug)	No zone	No zone

The enhanced %EE in these formulations could be due to the more efficient encapsulation of the active ingredients in the smaller particles, leading to less leakage and higher retention of the active compound.

Evaluation of Optimized Nanosponges

Mean particle diameter, surface charge (zeta potential), and distribution uniformity

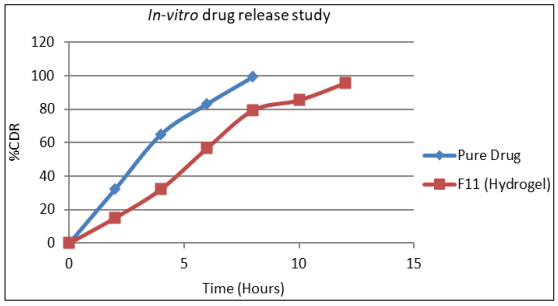

Figure 8: Release Pattern Analysis of Pure drug and Sulconazole-Loaded Nanosponges (F11)

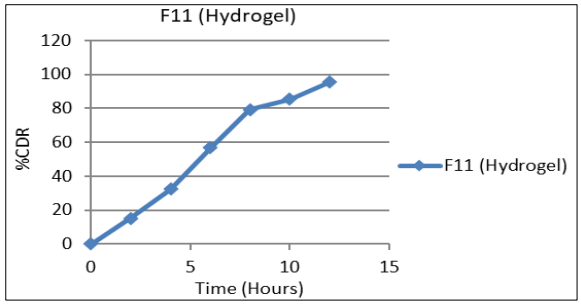

Figure 9: Release Pattern Analysis of Sulconazole-Loaded Nanosponges (F11)

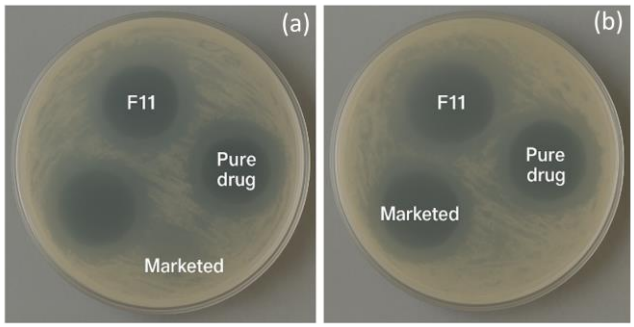

Figure 10: Zone of Inhibition: (a) *Candida albicans; (b) Aspergillus niger*

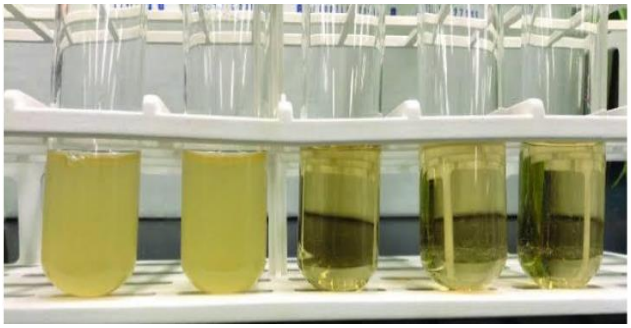

Figure 11: Broth Micro Dilution Assay

Table 12: Broth Micro Dilution Assay

Formulation	Concentration Range (µg/mL)	*Candida albicans*		*Aspergillus niger*	
		MIC (µg/mL)	MFC (µg/mL)	MIC (µg/mL)	MFC (µg/mL)
Sulconazole Nanosponges (F11)	0.0625 – 16	0.5	1.0	1.0	2.0
Pure Sulconazole	0.0625 – 16	1.0	2.0	2.0	4.0
Marketed Sulconazole Cream	0.0625 – 16	0.5	1.0	1.0	2.0

Particle Size, Zeta Potential and Polydispersity Index (PDI)

Figures 3 and 4 confirm that the F11 formulation produced well-dispersed nanoparticles averaging 265.7 nm in size, with a zeta potential of −23.54 mV and a PDI of 0.286, suggesting stable separation by repulsive interparticle forces.

% EE and Drug Loading Capacity (%DL)

As presented in Table 9, the %EE and %DL varied across all 13 formulations, reflecting the influence of polymer and surfactant concentrations. Among all batches, formulation F11 exhibited the highest %EE (86.24 ± 0.11%) and %DL (83.89 ± 0.17%), indicating optimal encapsulation and loading capacity. (Table 6).

FTIR and DSC Analysis

FTIR analysis of pure Sulconazole revealed characteristic peaks at 3042.86 cm^{-1} and 2991.56 cm^{-1} (C–H stretching), 1639.86 cm^{-1} (C=O bending), and 631 cm^{-1} and 768.99 cm^{-1} corresponding to imidazole and aromatic ring vibrations.

The physical mixture spectrum mirrored the pure drug, indicating no significant interactions and confirming drug–exipient compatibility. An endothermic peak for melting was observed at 127.90ºC on the DSC thermogram of the SUL pure substance. The nanosponges of SUL in the amorphous nanosponge core are indicated in Figure 6, as the endothermic peak of the nanosponge was 187.82ºC, which is in closer proximity to the peak of EC

SEM Analysis

As per the SEM analysis, the nanosponge Formulation (F1-F13) achieved particle size ranging from 251-365nm (Table 2). As shown in Figure 20, the nanosponge surface had no trace of any crystalline drug particles, and the particle diameters of all formulations remained constant.

In-vitro Drug Release Study

As shown in Table 11, the optimized nanosponge formulation (F11) exhibited a sustained drug release profile over 12 hours, reaching 98.03 ± 0.01% at the end of the study. In contrast, the pure drug showed a faster release, with 99.42 ± 0.06% released within 8 hours. These results confirm the extended release capability of the nanosponge system as shown in Table 7 and Figure 7.

Formulation of Hydrogel using Optimized Nanosponges

Using the emulsion solvent evaporation method, Sulconazole nanosponges (F11) were prepared with EC and PVA, then loaded into a hydrogel made from Carbopol 940. After soaking the gel base overnight, propylene glycol and the nanosponge dispersion were combined and stirred for 20 minutes at 400 rpm.

Evaluation of Sulconazole Nanosponges Hydrogel

Formulation F11 exhibited a pH of 6.21 ± 0.01 for the nanosponge dispersion and 5.85 ± 0.09 for the corresponding hydrogel, both within the acceptable range for topical application. The viscosity of the NS-based gel was found to be 1968 ± 2.19 cps, indicating suitable consistency for skin adherence and application (Table 8). As shown in Table 13, the optimized hydrogel formulation F11 exhibited a drug content of 91.41 ± 0.19% and a Spreadability of 93.49 ± 1.09%, indicating efficient drug incorporation and excellent ease of application suitable for topical delivery (Table 9).

In-vitro Release Study

The F11 Nanogel formulation demonstrated a prolonged drug release pattern, releasing 15.14 ± 1.36% at 2 hours and achieving 95.38 ± 2.96% by 12 hours (Table 10, Figure 9). These findings confirm extended-release behavior, with a steady increase in drug diffusion from the nanosponge-loaded hydrogel.

Agar Well Diffusion Method

As shown in Table 10 and Figure 10, the optimized Sulconazole nanosponge hydrogel (F11) produced the largest inhibition zones (21.3 ± 0.5 mm for *C. albicans* and 19.7 ± 0.6 mm for *A. niger*), outperforming the pure drug and marketed cream. The placebo exhibited no activity, confirming the drug-dependent antifungal effect.

Broth Micro Dilution Assay

The antifungal evaluation (Table [11], Figure [11]) revealed that formulation F11 exhibited MIC/MFC values of 0.5/1.0 µg/mL for *C. albicans* and 1.0/2.0 µg/mL for *A. niger*, demonstrating both fungistatic and fungicidal effects at clinically relevant concentrations.

CONCLUSION

The present study successfully developed a Sulconazole-loaded nanosponge hydrogel using a QbD-based optimization strategy. The optimized formulation (F11) exhibited nanosized particles with excellent entrapment efficiency, drug loading, and stability. Characterization through FTIR, DSC, and SEM confirmed the successful encapsulation of Sulconazole and its compatibility with excipients.

Characterization results confirmed that the hydrogel possessed ideal pH, viscosity, and spreadability parameters for skin application. Drug release profiles showed controlled, sustained release consistent with zero-order kinetics. The nanosponge hydrogel also exhibited superior antifungal effectiveness against *C. albicans* and *A. niger* when compared to the pure drug and a commercial cream. MIC and MFC studies confirmed both fungistatic and fungicidal potential of the formulation. Overall, this dual

drug delivery approach—combining nanosponges and hydrogel—proves to be a promising strategy for enhancing the therapeutic performance and patient compliance of topical antifungal treatments.

REFERENCES

1. Kaur IP, Kakkar S. Topical delivery of antifungal agents. *Expert Opin Drug Deliv*. 2010;7(12):1303–1327.
2. Barry BW. Dermatological formulations: percutaneous absorption. *Drugs Pharm Sci*. 1983;18:1–30.
3. Raza K, Singh B, Singla S, Wadhwa S, Katare OP. Lipid-based topical delivery of antifungal agent: design, characterization and comparison with conventional system. *Pharm Dev Technol*. 2013;18(1):64–72.
4. Nandhini M, Chinnasamy V, Ganesan M, Ramasamy S, Manavalan R. A comprehensive review on topical antifungal therapy. *J Drug Deliv Ther*. 2021;11(2-S):18–26.
5. Cevc G, Blume G. Lipid vesicles penetrate into intact skin owing to the transdermal osmotic gradients and hydration force. *Biochim Biophys Acta*. 1992;1104(1):226–232.
6. Vyas A, Saraf S. Topical delivery of antifungal agents: recent advances and future perspectives. *Chem Biol Lett*. 2013;20(3):220–226.
7. Sharma R, Dangi V, Nagpal M, Arora S, Ali J, Baboota S. Nanosponges: a novel drug delivery system. *J Drug Deliv Sci Technol*. 2021;61:102308.
8. Osmani RA, Aloorkar NH, Kulkarni AS, Hani U, Bhosale RR. Nanosponges: The spawning innovation in drug delivery systems. *J Drug Deliv Sci Technol*. 2014;24(6):385–391.
9. Hoare TR, Kohane DS. Hydrogels in drug delivery: Progress and challenges. *Polymer (Guildf)*. 2008;49(8):1993–2007.
10. Varuna U, Venkata N, Vidiyala N, Sunkishala P. Bio-Inspired Green Synthesis of Nanoparticles for Psoriasis Treatment : A Review of Current Status and Future Directions. Asian J Green Chem. 2025;9:373–403.
11. Subramanian S, Natesan S, Parthiban S, et al. In vitro antifungal activity of sulconazole nitrate-loaded nanoparticulate gel. Indian J Pharm Sci. 2021;83(3):437–443.
12. Raza K, Singh B, Singla S, Wadhwa S, Katare OP. Lipid-based topical delivery of antifungal agent: design, characterization and comparison with conventional system. Pharm Dev Technol. 2013;18(1):64–72.
13. Jain V, Singh R. Dendrimer: a novel carrier for drug delivery. J Indian Acad Clin Med. 2010;11(1):31–36.
14. Sireesha D, Teja RK, Padmabhushana CV. Quality-by-design approach for development of oxiconazole nitrate-loaded nanosponges for topical delivery. Future J Pharm Sci. 2022;8:1–11.
15. Trotta F, Zanetti M, Cavalli R. Cyclodextrin-based nanosponges as drug carriers. Beilstein J Nanotechnol. 2012;3:167–178.
16. Manchanda S, Sahoo PK. Development and evaluation of voriconazole-loaded nanosponges for oral and topical delivery. J Drug Deliv Sci Technol. 2021;66:102832.
17. Dayyih WA, Awad R. Revolutionizing drug development: The role of AI in modern pharmaceutical research. J Pharm Sci Comput Chem. 2025;1(1):206–27.
18. Sanna V, Gavini E, Cossu M, Rassu G, Giunchedi P. Solid lipid nanoparticles (SLN) as carriers for the topical delivery of econazole nitrate: in-vitro characterization, ex-vivo and in-vivo studies. J Pharm Pharmacol. 2007;59(8):1057–64
19. Balouiri M, Sadiki M, Ibnsouda SK. Methods for in vitro evaluating antimicrobial activity: A review. *J Pharm Anal*. 2016;6(2):71–79.
20. Mowat E, et al. Phase-dependent antifungal activity against *Aspergillus fumigatus* using a novel screening method. *J Med Microbiol*. 2008;57(Pt 5):614–622.
21. Ashindortiang OI, Anyama CA, Ayi AA. Phytosynthesis, Characterization and Antimicrobial Studies of Silver Nanoparticles Using Aqueous Extracts of Olax Subscorpioidea. Adv J Chem Sect A. 2022;5(3):215–25.
22. Odeh LU, Nnanyelugo CE, Adams A, Abubakar SA, Ejikeme CS, Igwe EP, et al. The synthesis and Characterization of Biobased Catalyst Derived from Palm Kernel Shell and Eggshell for the Production of Biodiesel. Adv J Chem Sect B, Nat Prod Med Chem. 2024;6(4):409–27.
23. Baraga WM, Shtewia FA, Ulsalam Tarrousha AA, Al-Adiwisha WM, Altounsib MK. Green Synthesis of Silver Nanowires Using Aqueous Brassica Tournefortii Leaves Extract and Evaluation of Their Antibacterial and Antioxidant Activities. J Appl Organomet Chem. 2025;5(1):13–27.
24. Hani U, Al-Qahtani EH, Albeeshi FF, Alshahrani SS. Exploring the Landscape of Drug-Target Interactions: Molecular Mechanisms, Analytical Approaches, and Case Studies. J Pharm Sci Comput Chem. 2025;1(1):12–25.
25. Dolatyari A, Nilchi A, Janitabardarzi S, Alipour A, Hashemi M. Evaluation of Ze/PAN Nanocomposites for Adsorption of Cs (I) from Aaqueous Environments. Chem Methodol. 2025;9(2):103–24.
26. Idan AH, Al-anbari HHA, Alhameedi DY, Khuder SA, Salah OH, Hashim AM, et al. Green and Eco-Friendly Synthesis of Hydrogel Biocomposites for Removal of Metal Ion from Aqueous Solution : Experimental , Quantum Chemical Parameters , and RDG. Asian J Green Chem. 2025;9:1–14.
27. Abd MI, Radia ND. Removal of Crystal Violet Dye from Aqueous Solutions Using a Xanthan Gum-Based Hydrogel Nanocomposite with TiO 2 Nanoparticles as an Eco-Friendly Green Surface. Asian J Green Chem. 2024;8:497–511.
28. CLSI. Reference Method for Broth Dilution Antifungal Susceptibility Testing of Yeasts; Approved Standard M27-A3. Wayne, PA: CLSI; 2008.

29. Pfaller MA, Diekema DJ. Progress in antifungal susceptibility testing of *Candida spp.* by CLSI methods. *J Clin Microbiol.* 2007;45(9):2846–2856.

30. Singh A, Chauhan CS. Formulation and Optimization of Valganciclovir-loaded Nanosponges. International Journal of Drug Delivery Technology. 2024;14(1):1-8.